Analysis of spatiotemporal signals: A method based on perturbation theory

A. Hutt,[1,*] C. Uhl,[1] and R. Friedrich[2]
[1]*Max-Planck-Institute of Cognitive Neuroscience, Stephanstrasse 1a, 04103 Leipzig, Germany*
[2]*Institute for Theoretical Physics, University of Stuttgart, Pfaffenwaldring 57, 70550 Stuttgart, Germany*
(Received 18 December 1998)

We present a method of analyzing spatiotemporal signals with respect to its underlying dynamics. The algorithm aims at the determination of spatial modes and a criterion for the number of interacting modes. Simultaneously, a way of filtering of nonorthogonal noise is shown. The method is discussed by examples of simulated stable fixpoints and the Lorenz attractor. [S1063-651X(99)01908-X]

PACS number(s): 05.45.−a, 02.50.Sk

I. INTRODUCTION

In various scientific fields the analysis of spatiotemporal patterns emerging from complex systems plays an important role. An investigation of measured multidimensional data allows us to learn more about the internal dynamics of the system. It represents the basis for microscopic modeling of interactions in investigated systems (e.g., [1]). Some typical fields of application are chemical reactions [2], meteorology (e.g., [3]) and hydrodynamics [4] or biological systems as analyzing electroencephalography (EEG) or magnetoencephalography (MEG) data [5–7].

Depending on the intended use, different kinds of data processing techniques can be applied. An often used method for linear data analysis is known as principal component analysis (PCA) [8] or Karhunen-Loève expansion. Spatial modes are calculated based on maximizing signal projections on these modes. It leads to orthogonal spatial and temporal modes and gives a measure for the contribution of each mode to the signal. Modes with a signal contribution above a certain threshold are considered as relevant, those below the threshold as irrelevant. However, this method fails to separate signal from noise, if signal and noise are not orthogonal on each other, and if noise parts contribute more than parts of the relevant signal to the data. Furthermore an estimation of the number of interacting modes depends on the choice of the threshold. Underlying dynamic structures are neglected by this linear data technique.

A nonlinear approach aiming at extracting interacting modes and the underlying dynamics has been presented, e.g., in [9,10]. However, the numerical effort of these nonlinear approaches is considerably high, especially with an increasing dimensionality of the underlying dynamical system. An estimation of the number of interacting modes is also still an open question.

In this paper we will present a nonlinear technique based on (linear) perturbation theory, which focuses on internal deterministic dynamic patterns and extracts signal dynamics from noisy data sets. It improves PCA suspending the condition of orthogonality and allows an objective estimation of interacting spatial modes. Due to the linear equations to be solved, the method leads to a fast and robust algorithm.

The perturbational approach is based on a ground state of the PCA modes, which represents the exact solution of minimizing a cost function leading to a complete orthogonal basis. We introduce a perturbation by an additional term in the cost function for a determination of signal dynamics. Using a mathematical methodology similar to Hartree and Fock [11,12], we obtain dynamically coupled spatial modes. A criterion for the estimation of the number of interacting modes can be derived. We obtain the relevant signal subspace independent of an orthogonality relation between signal and noise, due to our special choice of a biorthogonal basis.

II. METHOD

A. Principal component analysis (PCA)

A N-dimensional spatiotemporal signal can be described by a vector $\mathbf{q}(t)$ of dimension N. In order to determine significant parts of the signal, one can decompose the signal into spatial and temporal modes $\mathbf{v}_i$ and $x_i(t)$ by PCA. The properties are determined by a cost function

$$V=\sum_{i=1}^{N}\frac{\langle[\mathbf{q}(t)-(\mathbf{q}\cdot\mathbf{v}_i)\mathbf{v}_i]^2\rangle}{\langle\mathbf{q}^2\rangle}+\sum_{i,j=1}^{N}\tau_{ij}(\mathbf{v}_i\cdot\mathbf{v}_j-\delta_{ij}),$$

$$\frac{\partial V}{\partial\mathbf{v}_k}=0, \tag{2.1}$$

where $\langle\cdots\rangle$ denotes time average and τ_{ij} are Lagrange multipliers to fulfill the orthogonality constraint.

Standard cost functions of PCA lead to degenerated solution spaces. To obtain the known equations of PCA directly, here one sums up the single errors to the signal and fixes the amplitudes as projections on the modes. This breaks the invariance with respect to linear transformation.

It leads to an eigenvalue problem

$$\mathbf{C}\mathbf{v}_k=\lambda_k\mathbf{v}_k, \tag{2.2}$$

with $\mathbf{C}=\langle\mathbf{q}(t)\otimes\mathbf{q}(t)\rangle/\langle\mathbf{q}^2\rangle$, orthogonal spatial modes $\mathbf{v}_k$ and amplitudes $x_k(t)=\mathbf{q}(t)\cdot\mathbf{v}_k$, where $\otimes$ denotes the dyadic product. They obey Eqs. (2.3),

$$\mathbf{v}_k\cdot\mathbf{v}_l=\delta_{kl}, \quad \langle x_k(t)x_l(t)\rangle=\lambda_k\delta_{kl}. \tag{2.3}$$

*Electronic address: hutt@cns.mpg.de

Since $V=N-\Sigma_i\lambda_i$, the modes are sorted with respect to their contribution to the signal given by the eigenvalues λ_i:

$$\lambda_1>\lambda_2>\cdots>\lambda_N. \tag{2.4}$$

By choosing a threshold λ_c and considering modes $\mathbf{v}_i$ with $\lambda_i>\lambda_c$ one obtains a subspace of the signal

$$\mathbf{q}(t)\simeq\sum_{i=1}^{M<N} x_i(t)\mathbf{v}_i. \tag{2.5}$$

The following problems arise by such an approach: (i) The choice of λ_c and, therefore, an estimation of the number of interacting modes is an open question. (ii) Noisy parts of the signal can be represented by modes $\mathbf{v}_i$ with $\lambda_i>\lambda_c$ and/or dynamically relevant modes $\mathbf{v}_j$ can be neglected because of $\lambda_j<\lambda_c$. (iii) If signal and noise are not orthogonal, the separation of signal from noise cannot be achieved by an orthogonal expansion.

B. Perturbational approach

To improve PCA with respect to these points, a biorthogonal base $\{\mathbf{w}_i^+\},\{\mathbf{w}_i\}$ with

$$\mathbf{w}_i^+\cdot\mathbf{w}_j=\delta_{ij},\quad \mathbf{w}_i\cdot\mathbf{w}_i=1 \tag{2.6}$$

is introduced. Amplitudes $x_k(t)$ are now obtained by the signal projection $x_i(t)=\mathbf{q}\mathbf{w}_i^+$.

A second extension is done by introducing an additional term $V_d(\mathbf{w}_i^+,\mathbf{w}_j,a_{i\alpha})$ in the cost function considering the dynamics of the signal. Since nonlinear interactions are assumed, V_d will depend nonlinearly on $\mathbf{w}_i^+$. In this paragraph the actual definition is irrelevant; it is sufficient to introduce parameters $a_{i\alpha}$ as parameters of the dynamic fit. The exact specification of the cost function V_d will be given in the next section.

We can interpret V_d as a perturbation of the groundstate built by PCA modes. Considering also the constraints (2.6) we define the cost function V as

$$V=\sum_{i=1}^{M}\frac{\langle[\mathbf{q}(t)-(\mathbf{q}\cdot\mathbf{w}_i^+)\mathbf{w}_i]^2\rangle}{\langle\mathbf{q}^2\rangle}+\epsilon V_d(\mathbf{w}_i^+,\mathbf{w}_j,a_{i\alpha})+\sum_{i,j=1}^{M}\tau_{ij}(\mathbf{w}_i^+\cdot\mathbf{w}_j-\delta_{ij})+\sum_{i=1}^{M}\alpha_i[(\mathbf{w}_i)^2-1]. \tag{2.7}$$

The parameter ϵ is a measure for perturbation of the PCA state, and τ_{ij} and α_i are Lagrangian parameters of the introduced constraints.

The minimum of the cost function V represents the dynamically relevant subspace spanned by the biorthogonal basis $\{\mathbf{w}_i^+\},\{\mathbf{w}_i\}$ of dimension $M\leqslant N$ in the given N-dimensional vector space. As $\mathbf{w}_i^+$, $\mathbf{w}_j$, $a_{i\alpha}$, τ_{kl}, and α_k are independent of each other, the minimum is obtained by vanishing partial derivatives of V:

$$\frac{\partial V}{\partial\mathbf{w}_k^+}=\mathbf{0},\quad \frac{\partial V}{\partial\mathbf{w}_k}=\mathbf{0}, \tag{2.8}$$

$$\frac{\partial V}{\partial a_{k\alpha}}=0, \tag{2.9}$$

$$\frac{\partial V}{\partial\tau_{kl}}=0,\quad \frac{\partial V}{\partial\alpha_k}=0. \tag{2.10}$$

Inserting Eq. (2.7) into Eqs. (2.8) and (2.10), we get

$$-2\mathbf{C}\mathbf{w}_k+2\mathbf{C}\mathbf{w}_k^++\epsilon\frac{\partial V_d}{\partial\mathbf{w}_k^+}+\sum_{j=1}^{M}\tau_{kj}\mathbf{w}_j=\mathbf{0}, \tag{2.11}$$

$$-2\mathbf{C}\mathbf{w}_k^++2(\mathbf{w}_k^+\mathbf{C}\mathbf{w}_k^+)\mathbf{w}_k+\epsilon\frac{\partial V_d}{\partial\mathbf{w}_k}+\sum_{i=1}^{M}\tau_{ik}\mathbf{w}_i^++2\alpha_k\mathbf{w}_k=\mathbf{0}, \tag{2.12}$$

$$\mathbf{w}_k^+\cdot\mathbf{w}_l=\delta_{kl}, \tag{2.13}$$

$$\mathbf{w}_k^2=1. \tag{2.14}$$

Because of the nonlinear dependence of $\partial V_d/\partial\mathbf{w}_k^+$ and $\partial V_d/\partial\mathbf{w}_k$, Eqs. (2.11) and (2.12) cannot be solved directly. Therefore, a perturbational approach is chosen: the modes are expanded by power series in ϵ,

$$\mathbf{w}_i^+=\mathbf{v}_i+\epsilon\mathbf{w}_i^{+(1)}+\epsilon^2\mathbf{w}_i^{+(2)}+\cdots, \tag{2.15}$$

$$\mathbf{w}_i=\mathbf{v}_i+\epsilon\mathbf{w}_i^{(1)}+\epsilon^2\mathbf{w}_i^{(2)}+\cdots, \tag{2.16}$$

as well as the Lagrangian parameters

$$\tau_{ij}=\tau_{ij}^0+\epsilon\tau_{ij}^1+\epsilon^2\tau_{ij}^2+\cdots, \tag{2.17}$$

$$\alpha_i=\alpha_i^0+\epsilon\alpha_i^1+\epsilon^2\alpha_i^2+\cdots. \tag{2.18}$$

The eigenvalues λ_i are not expanded; the amplitudes $x_i(t)$ remain the projections of the signal on the expanded modes $\mathbf{w}_i^+$. The expansion coefficients $\mathbf{w}_i^{+(n)}$ and $\mathbf{w}_i^{(n)}$ are built by superposition of the PCA modes $\mathbf{v}_i$,

$$\mathbf{w}_i^{+(n)}=\sum_{j=1}^{N}c_{ij}^n\mathbf{v}_j,\quad \mathbf{w}_i^{(n)}=\sum_{j=1}^{N}d_{ij}^n\mathbf{v}_j. \tag{2.19}$$

Finally, the terms of Eqs. (2.11) and (2.12) can be sorted with respect to powers of ϵ and evaluated separately.

1. Ground state

First we investigate the solution in perturbation order $n=0$. With Eqs. (2.15) and (2.16) it follows that

$$\tau_{kl}^0=0,\quad \alpha_k^0=0. \tag{2.20}$$

Equation (2.12) leads to

$$\mathbf{C}\mathbf{v}_k=\lambda_k^0\mathbf{v}_k, \tag{2.21}$$

$$\langle x_l(t)x_k(t)\rangle=\lambda_k\delta_{lk}, \tag{2.22}$$

with $x_k(t)$ representing amplitudes of PCA. As constructed, the ground state corresponds to the PCA solution.

2. First-order perturbation

In the first-order perturbation, we have to deal with nonquadratic coefficient tensors $\{c^n_{km}\}$ and $\{d^n_{km}\}$ with $1 \leqslant k \leqslant M$, $1 \leqslant m \leqslant N$.

First we investigate the case $1 \leqslant k \leqslant M$ and $1 \leqslant m \leqslant M$ and obtain from evaluating Eq. (2.6):

$$d^1_{km} = -c^1_{mk}, \quad d^1_{kk} = c^1_{kk} = 0. \tag{2.23}$$

Equations (2.11) and (2.12) lead to Lagrangian parameters,

$$\alpha^1_k = -\left.\frac{\partial V_d}{\partial \mathbf{w}_k}\right|_0 \cdot \mathbf{v}_k + \left.\frac{\partial V_d}{\partial \mathbf{w}^+_k}\right|_0 \cdot \mathbf{v}_k, \quad \tau^1_{kk} = -\left.\frac{\partial V_d}{\partial \mathbf{w}^+_k}\right|_0 \cdot \mathbf{v}_k, \tag{2.24}$$

$$\tau^1_{km} = \frac{\lambda^0_m}{(\lambda^0_k - \lambda^0_m)}(\Delta_{mk} - \Delta_{km}) - \left.\frac{\partial V_d}{\partial \mathbf{w}^+_k}\right|_0 \cdot \mathbf{v}_m \quad \forall \quad k \neq m, \tag{2.25}$$

and coefficients

$$c^1_{km} = \frac{1}{(\lambda^0_k - \lambda^0_m)^2}\left(\frac{1}{2}(\lambda^0_k + \lambda^0_m)\Delta_{km} - \lambda^0_k \Delta_{mk}\right) \quad \forall k \neq m \tag{2.26}$$

with

$$\Delta_{km} = \left.\frac{\partial V_d}{\partial \mathbf{w}^+_m}\right|_0 \cdot \mathbf{v}_k - \left.\frac{\partial V_d}{\partial \mathbf{w}_k}\right|_0 \cdot \mathbf{v}_m. \tag{2.27}$$

The terms $\partial V_d / \partial \mathbf{w}^+_m|_0$ and $\partial V_d / \partial \mathbf{w}_m|_0$ represent partial derivatives with $\mathbf{w}^+_k = \mathbf{w}_k = \mathbf{v}_k$.

In the case of $1 \leqslant k \leqslant M$ and $M < m \leqslant N$, we get

$$c^1_{km} = -\frac{1}{2\lambda^0_m(\lambda^0_k - \lambda^0_m)}\left(\lambda^0_m \left.\frac{\partial V_d}{\partial \mathbf{w}_k}\right|_0 \cdot \mathbf{v}_m + \lambda^0_k \left.\frac{\partial V_d}{\partial \mathbf{w}^+_k}\right|_0 \cdot \mathbf{v}_m\right), \tag{2.28}$$

$$d^1_{km} = -\frac{1}{2(\lambda^0_k - \lambda^0_m)}\left(\left.\frac{\partial V_d}{\partial \mathbf{w}_k}\right|_0 \cdot \mathbf{v}_m + \left.\frac{\partial V_d}{\partial \mathbf{w}^+_k}\right|_0 \cdot \mathbf{v}_m\right), \tag{2.29}$$

and the Lagrangian parameters vanish.

In this paper we are dealing with low-dimensional dynamics; however, in the case of high-dimensional dynamics, the denominator $(\lambda^0_k - \lambda^0_m)$ may become small for high numbers k,l and, therefore, perturbation theory in degenerated states should be applied.

C. Specification of V_d

So far we have not specified the cost function V_d considering dynamic interactions. Our choice relies on the PCA approach for the time derivative of the signal,

$$\sum_{i=1}^{M} \frac{\langle (\dot{\mathbf{q}} - \dot{x}_i \mathbf{w}_i)^2 \rangle}{\langle \dot{\mathbf{q}}^2 \rangle}. \tag{2.30}$$

Because of the assumed interactions, the time derivative of the amplitudes $\dot{x}_i(t)$ can be described as a function of x_j,

$$\dot{x}_i = f_i[x_j]. \tag{2.31}$$

Inserting this expression into Eq. (2.30), we obtain our definition of the cost function V_d:

$$V_d = \sum_{i=1}^{M} \frac{\langle (\dot{\mathbf{q}} - f_i \mathbf{w}_i)^2 \rangle}{\langle \dot{\mathbf{q}}^2 \rangle}. \tag{2.32}$$

The time derivative of $\mathbf{q}(t)$ is calculated numerically and remains regular in the case of weak noise. Strong noise can lead to irregular numerical values, which need to be investigated separately.

As an ansatz for the function $f_i[x_j]$ we choose a polynomial function,

$$f_i[x_j] = \sum_{j=1}^{M} \Gamma^1_{ij} x_j + \sum_{j=1}^{M} \sum_{k=1}^{j} \Gamma^2_{ijk} x_j x_k + \sum_{j=1}^{M} \sum_{k=1}^{j} \sum_{l=1}^{k} \Gamma^3_{ijkl} x_j x_k x_l, \tag{2.33}$$

since most of the generic cases can be modeled by such a set of differential equations. To abbreviate the notation, we can define a vector $\{\xi_\alpha\}$ consisting of the powers of x_i,

$$\{\xi_\alpha\} = \{x_1, x_2, \ldots, x_M, x_1^2, x_1 x_2, \ldots, x_M^2, x_1^3, x_1^2 x_1, \ldots, x_M^3\}, \tag{2.34}$$

and summarize Eq. (2.33) to

$$f_i[x_j] = \sum_\alpha a_{i\alpha} \xi_\alpha. \tag{2.35}$$

The derivatives $\partial V_d / \partial \mathbf{w}_k|_0$ and $\partial V_d / \partial \mathbf{w}^+_k|_0$ occurring in the expressions of coefficients c^1_{km} can now be evaluated to

$$\left.\frac{\partial V_d}{\partial \mathbf{w}_k}\right|_0 = \frac{2}{\langle \dot{\mathbf{q}}^2 \rangle} \sum_\alpha \left(\sum_\beta a^0_{k\beta} M_{\alpha\beta} \mathbf{v}_k - \langle \xi^0_\alpha \dot{\mathbf{q}} \rangle\right) a^0_{k\alpha}, \tag{2.36}$$

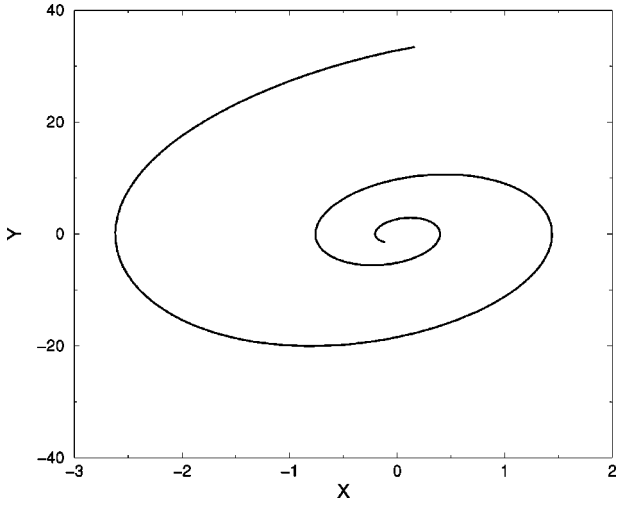

FIG. 1. Trajectory near a stable fixpoint in the x-y plane.

$$\left.\frac{\partial V_d}{\partial \mathbf{w}_k^+}\right|_0 = \frac{2}{\langle \dot{\mathbf{q}}^2 \rangle} \sum_{i=1}^{M} \sum_{\beta} \left\langle \left(\sum_{\alpha} a_{i\alpha}^0 \xi_\alpha^0 - \dot{\mathbf{q}} \cdot \mathbf{v}_i \right) a_{i\beta}^0 \frac{\partial \xi_\beta^0}{\partial \mathbf{w}_k^+} \right\rangle . \tag{2.37}$$

Thereby, the polynomial coefficients $a_{k\alpha}^0$ are obtained from Eq. (2.9) as

$$a_{k\alpha}^0 = \sum_{\beta} b_{k\beta} M_{\beta\alpha}^{-1} \tag{2.38}$$

with

$$b_{k\beta} = \langle (\mathbf{q} \cdot \mathbf{v}_k) \xi_\beta^0 \rangle, \quad M_{\alpha\beta} = \langle \xi_\alpha^0 \xi_\beta^0 \rangle, \tag{2.39}$$

and the derivatives of ξ_β^0 are given as

$$\xi_\beta^0 = x_r : \frac{\partial \xi_\beta^0}{\partial \mathbf{w}_k^+} = \mathbf{q} \delta_{rk},$$

$$\xi_\beta^0 = x_r x_s, \quad r \leqslant s : \frac{\partial \xi_\beta^0}{\partial \mathbf{w}_k^+} = \mathbf{q}(\delta_{kr} x_s + \delta_{ks} x_r), \tag{2.40}$$

$$\xi_\beta^0 = x_r x_s x_t,$$

$$r \leqslant s \leqslant t : \frac{\partial \xi_\beta^0}{\partial \mathbf{w}_k^+} = \mathbf{q}(\delta_{kr} x_s x_t + \delta_{ks} x_r x_t + \delta_{kt} x_r x_s).$$

D. Dynamically relevant subspace

Assuming a M-mode interaction, the modes $\mathbf{w}_i^+, \mathbf{w}_i$ given by Eqs. (2.15), (2.16), and (2.19) are calculated in first-order correction out of M PCA modes. In the N-dimensional signal space, there are $\binom{N}{M}$ possible combinations to choose M out of N PCA modes as the ground state. Therefore, we obtain $\binom{N}{M}$ alternatives improving the corresponding PCA modes. Since the cost function V_d measures dynamics representation, the best estimation of the relevant subspace is spanned by modes $\mathbf{w}_k^+, \mathbf{w}_k$ with minimal value of $V_d(\mathbf{w}_k^+, \mathbf{w}_k, \epsilon, M)$, i.e., by investigation of $\Sigma_{M=1}^{N} \binom{N}{M}$ branches, the best choice of spatial modes (in first-order perturbation theory) spanning the dynamically relevant subspace and the number of interacting modes is obtained.

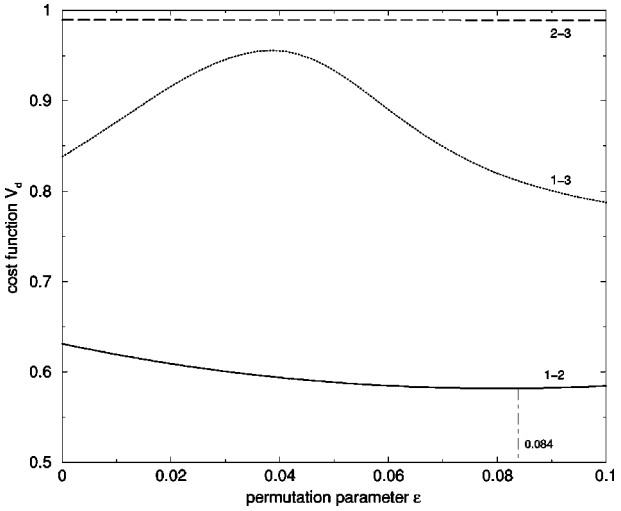

FIG. 2. Calculated cost function $V_d(M=2,\epsilon)$ for the signal near a stable fixpoint. The plot shows a minimum with a combination of the first two PCA modes (solid line) at $\epsilon_{min}=0.084$. The dotted line corresponds to the combination of PCA modes 1 and 3; the dashed line corresponds to the combination of PCA modes 2 and 3.

III. APPLICATIONS TO SIMULATED DATA SETS

To illustrate our approach we will present in the following the analysis of three simulated data sets consisting of two-mode interactions with one- and three-dimensional noise orthogonal to the signal, and a chaotic three-mode interaction, with additive noise nonorthogonal to the signal.

A. Noisy signal near a stable fixed point

First we assume a three-dimensional spatiotemporal signal near a two-dimensional stable fixed point and additive orthogonal noise,

$$\mathbf{q}(t) = x(t) \begin{pmatrix} 10 \\ 0 \\ 0 \end{pmatrix} + y(t) \begin{pmatrix} 0 \\ 1 \\ 0 \end{pmatrix} + nz(t) \begin{pmatrix} 0 \\ 0 \\ 1 \end{pmatrix}. \tag{3.1}$$

The amplitudes $x(t)$ and $y(t)$ thereby obey the following set of differential equations:

$$\dot{x} = -y,$$

$$\dot{y} = ax + by + cx^2 y, \tag{3.2}$$

where $a=0.06$, $b=-0.1$, $c=0.01$, $x(t_0)=0.3$, and $y(t_0)=0.7$. The noise amplitude $z(t)$ is modeled by

$$z(t) = \mathcal{N} \sum_{i=1}^{\eta} \rho_i(t) G_i(\mu_i, \sigma_i^2, t). \tag{3.3}$$

Here $\rho_i \in [-0.5;0.5]$ and $\eta \in [0;T]$ denote random numbers, T denotes the number of time steps, and $G_i(\mu_i, \sigma_i^2, t)$ represent temporal Gaussian functions with random means

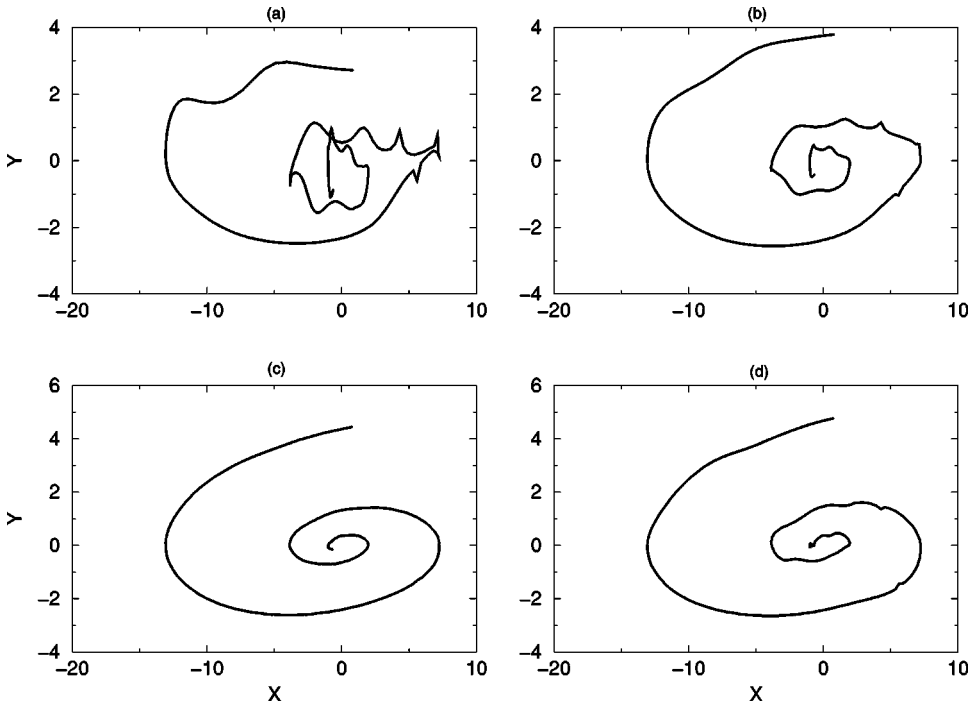

FIG. 3. Projected trajectories in the plane spanned by new modes $\mathbf{w}_1^+, \mathbf{w}_2^+$. The perturbation parameter ϵ is varied from $\epsilon = 0.000$ (a) over $\epsilon = 0.052$ (b) and $\epsilon = 0.084$ (c) to $\epsilon = 0.100$ (d). We recognize the best projection in (c), as predicted by Fig. 2.

μ_i and random variances σ_i^2. The factor $\mathcal{N}$ is introduced to scale $z(t)$ to $\langle z^2(t)\rangle = 1$, n in Eq. (3.1) allows tuning the signal-to-noise ratio.

Figure 1 shows the signal in x–y plane: the trajectory cycles into a stable fixed point.

We investigate the three-dimensional ($N=3$) data set considering $M=2$ interacting modes. Thus, we deal with $\binom{3}{2}$ branches of ground states: PCA modes 1 and 2, modes 1 and 3, and modes 2 and 3. The corresponding values of the cost function V_d are plotted in dependence of ϵ in Fig. 2. The branch of PCA modes 1 and 2 represents the best dynamic fit; they capture most of the dynamics. From the figure we expect the best improvement of the PCA modes for a perturbation value of $\epsilon_{min} = 0.084$. This effect of the perturbation by the nonlinear cost function V_d is illustrated in Fig. 3: the projections $x(t) = \mathbf{w}_1^+ \cdot \mathbf{q}(t)$ and $y(t) = \mathbf{w}_2^+ \cdot \mathbf{q}(t)$ are presented in the x-y phase space for different values of ϵ. In agreement with our expectations from Fig. 2, the best fit compared to Fig. 1 is obtained for $\epsilon = \epsilon_{min}$, with a dramatic improvement compared to the PCA solution ($\epsilon = 0$).

The influence of the noisy part of the signal is investigated by varying the scaling n of the noise amplitude. Figure 4 presents the results by plots of $V_d(M=2,\epsilon)$. Increasing signal-noise ratio s/n, defined by $s/n = \sqrt{\langle \mathbf{q}_{signal}^2 \rangle / \langle \mathbf{q}_{noise}^2 \rangle}$, decreases the quality of the fit by increasing values of V_d and increases ϵ_{min}, i.e., for higher noise levels the influence of our additional cost function V_d becomes more important, which is reflected by increasing values of ϵ_{min}. For high noise levels the

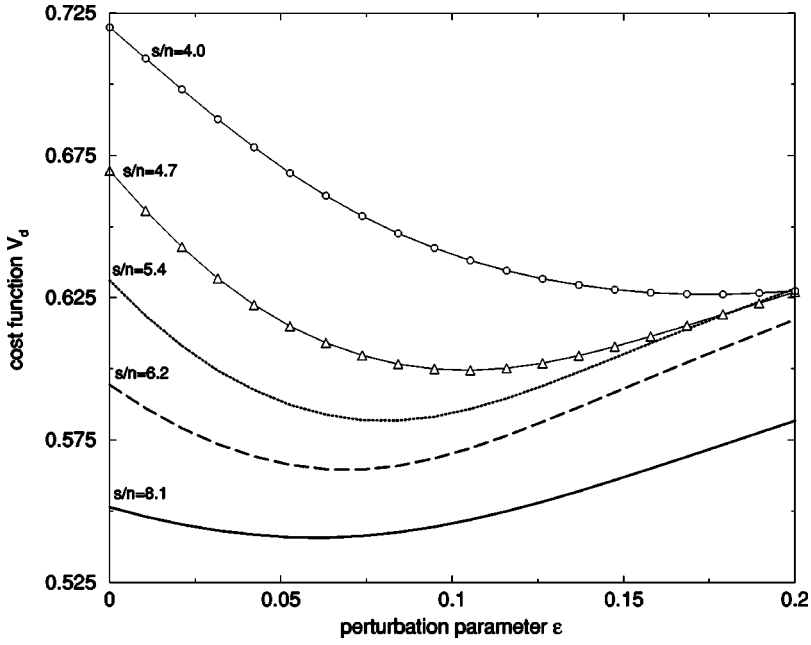

FIG. 4. Cost function $V_d(\epsilon)$ for different values of the signal-to-noise ratio s/n.

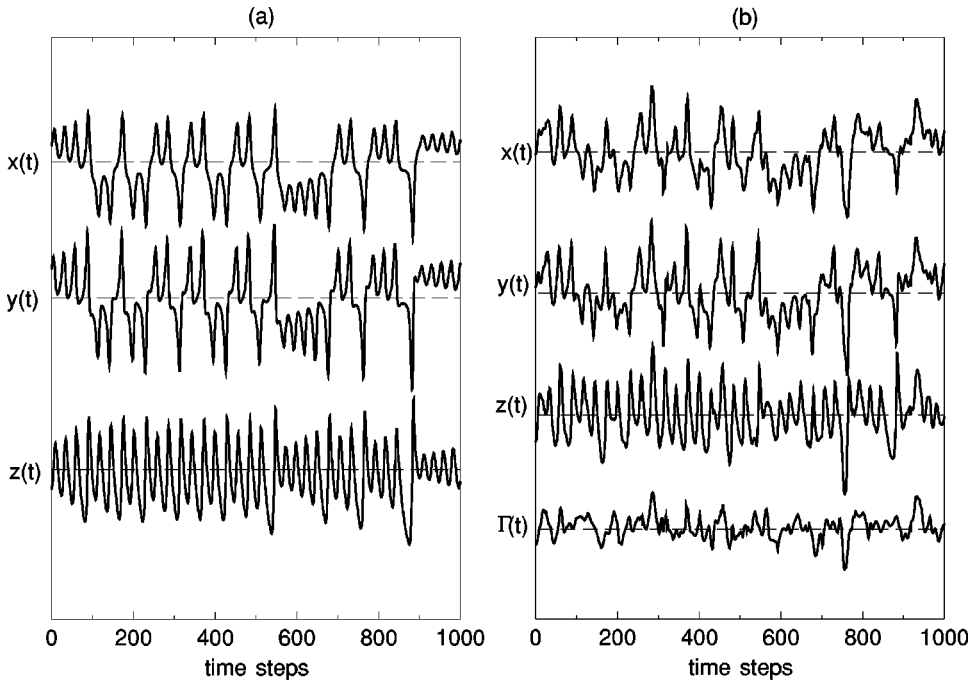

FIG. 5. Amplitudes of the Lorenz attractor without noise (a) and with nonorthogonal noise where a channel with pure noise is added in an additional dimension (b).

first-order perturbation may not be sufficient to capture most of the dynamics, higher-order perturbation terms may be considered.

B. Noisy Lorenz attractor

The second example deals with a four-dimensional signal $\mathbf{q}(t)$, consisting of a three-mode chaotic signal $[x(t),y(t),z(t)]$ and additive nonorthogonal noise,

$$\mathbf{q}(t)=x(t)\begin{pmatrix}1\\0\\0\\0\end{pmatrix}+y(t)\begin{pmatrix}0\\1\\0\\0\end{pmatrix}+z(t)\begin{pmatrix}0\\0\\1\\0\end{pmatrix}+\Gamma(t)\begin{pmatrix}1\\1\\1\\1\end{pmatrix}. \tag{3.4}$$

The chaotic signal is modeled by the Lorenz equations,

$$\dot{x}=-\sigma(x-y)+\alpha(t), \tag{3.5}$$

$$\dot{y}=rx-y-xz+\alpha(t),$$

$$\dot{z}=-bx+xy+\alpha(t),$$

with $\sigma=10$, $r=2.8$, $b=8/3$, $x(t_0)=0.1$, $y(t_0)=0.2$, and $z(t_0)=0.3$.

The noise amplitude $\Gamma(t)$ is modeled by

$$\Gamma(t)=\mathcal{N}\sum_{i=1}^{\eta}\rho_i(t)G_i(\mu_i,\sigma_i^2,t), \tag{3.6}$$

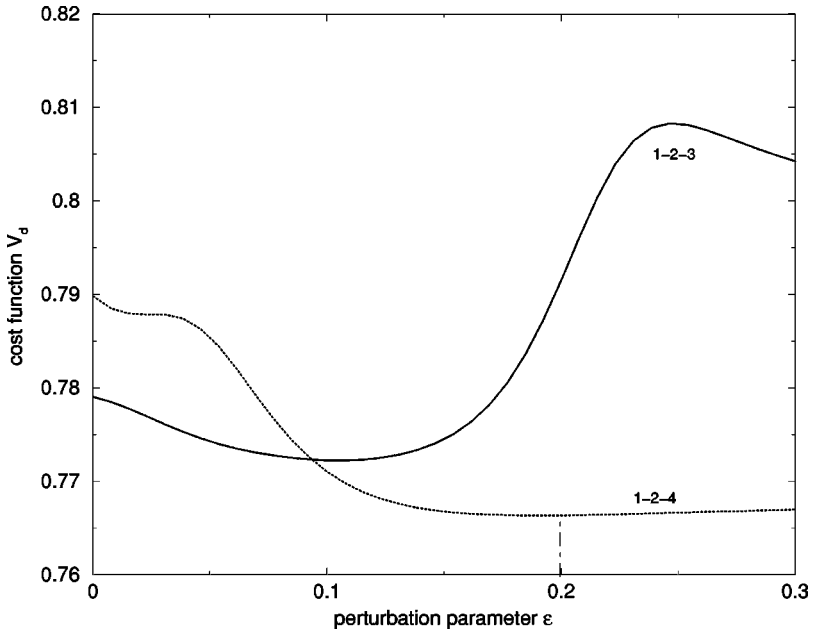

FIG. 6. Dynamic cost function for the Lorenz signal with respect to the perturbation parameter ϵ with number of interacting modes $M=3$. The deepest minimum is observed at $\epsilon=0.2$ with a combination of PCA modes 1, 2, and 4 (dotted line). The solid line corresponds to the combination of PCA modes 1, 2, and 3.

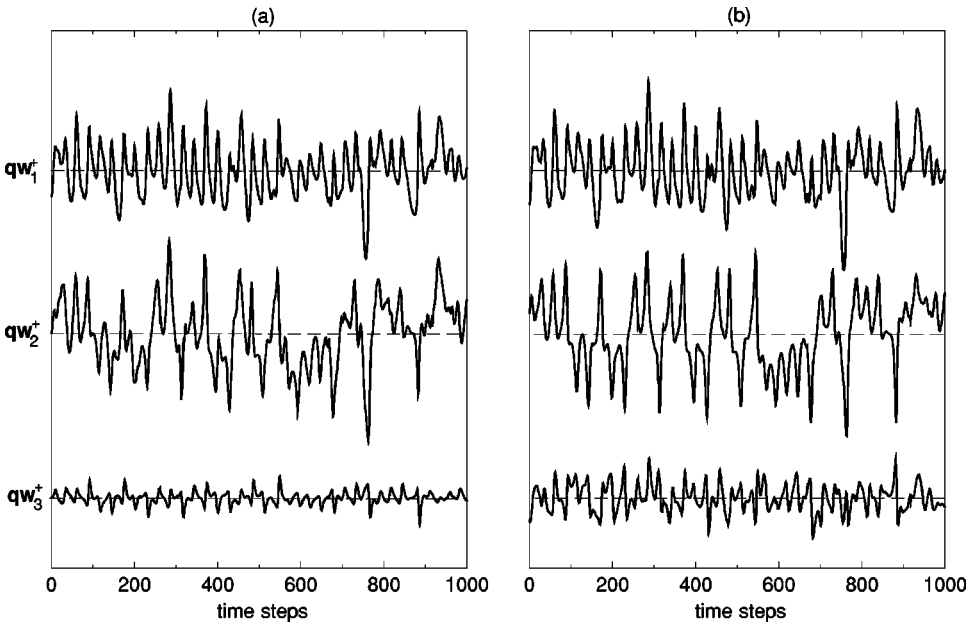

FIG. 7. Amplitudes $\mathbf{q}\cdot\mathbf{w}_i^+$ obtained by the PCA fit (a) and our perturbational approach (b).

with the same abbreviations as in the example above; α denotes correlated low noise. In Fig. 5(a) the amplitudes of the ''pure'' three-mode interaction without noise, $x(t)$, $y(t)$, and $z(t)$, are presented. Fig. 5(b) shows the four-dimensional spatiotemporal signal $\mathbf{q}(t)$, as given by Eq. (3.4).

We investigate the simulated signal by assuming a three-mode interaction. Therefore, we deal with $\binom{4}{3}$ PCA ground states and corresponding branches V_d. Figure 6 shows two branches (corrections based on PCA modes 1, 2, and 3, as well as based on modes 1, 2, and 4), the other two omitted branches are considerably higher. One observes that corrections of the 1–2–4 PCA ground state lead to better dynamics representation as the 1-2-3 combination, i.e., in the third PCA mode there is a higher contribution of the noisy part than of the deterministic part, whereas in the fourth PCA mode the deterministic part overbalances the noisy contribution. This behavior is corrected by our approach, in such a way that the separation of the deterministic—even though chaotic—part from the noisy part is improved.

Figure 7 presents the PCA amplitudes in comparison to the amplitudes obtained by our algorithm at $\epsilon=\epsilon_{min}$.

A comparison of both results to the deterministic signal $\mathbf{y}$ is shown in Fig. 8. Here we transformed the original deterministic signal part $\mathbf{x}=(x,y,z)^t,\Gamma(t)=0$ by a transformation matrix $\mathbf{L}$ to neglect any scaling effects due to different orientations or scales of the compared signals.

$\mathbf{L}$ is determined by

$$\frac{\partial}{\partial L_{kl}}\langle[\mathbf{y}(t)-\mathbf{L}\mathbf{x}(t)]^2\rangle=0 \tag{3.7}$$

$$\rightarrow L_{kl}=\sum_j \langle y_k x_j\rangle\langle x_j x_l\rangle^{-1}. \tag{3.8}$$

The improvement obtained by our algorithm compared to the PCA approach can be clearly observed in Fig. 8.

C. Estimation of the number of interacting modes

We simulate a five-dimensional signal $\mathbf{q}(t)=(x(t),y(t),\Gamma_1(t),\Gamma_2(t),\Gamma_3(t))^T$ based on the two-mode interaction given by Eq. (3.2) and orthogonal noise given by normalized amplitudes,

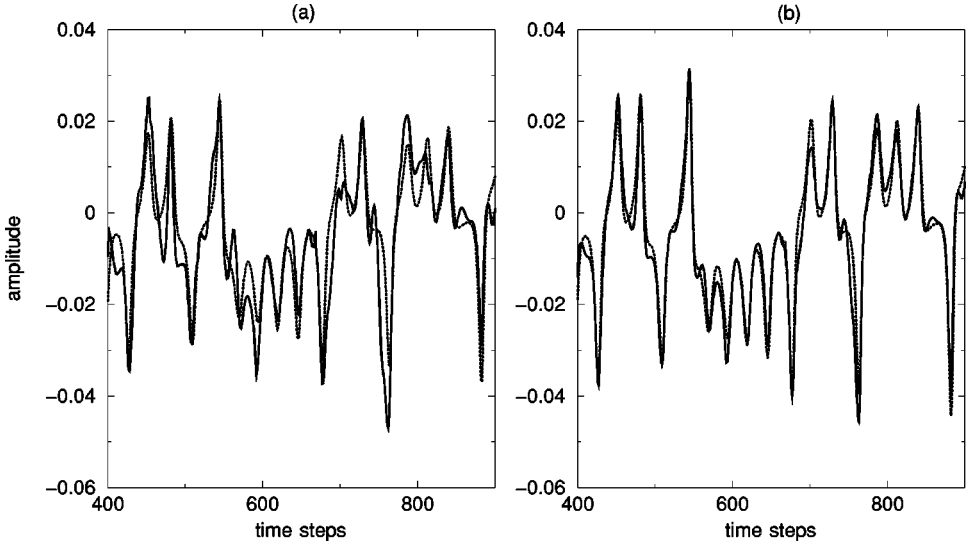

FIG. 8. A direct comparison of deterministic (dotted line) and reconstructed signals (solid line). The best PCA fit is shown in (a), the best perturbation fit in (b), where a better match can be recognized. We cut off parts of the time window to improve the comparison.

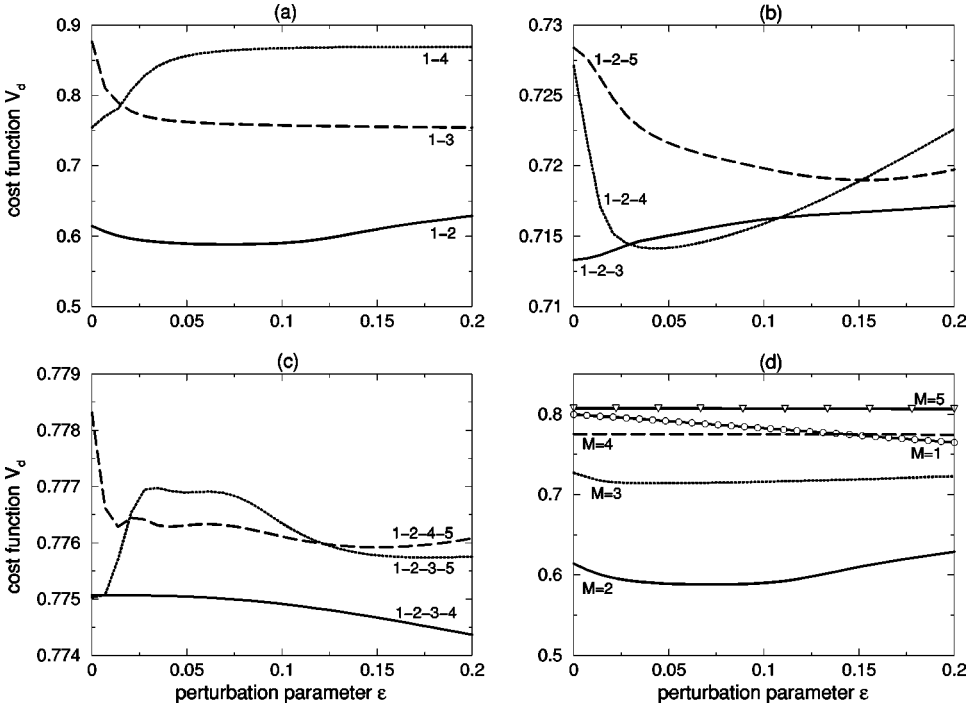

FIG. 9. Dynamic cost functions $V_d(M,\epsilon)$ calculated for the noisy signal near a stable fixpoint. Only combinations m-n of PCA modes yielding the deepest minimum of V_d are shown for various numbers of interacting modes: $M=2$ in (a), $M=3$ in (b), and $M=4$ in (c). In (d), a comparison of the best fits of all M interacting modes is presented. We recognize an obvious best fit at $M=2$. The cases where $M=1$ and $M=5$ were not plotted with different PCA ground states because of their visible irrelevance to the result in (d).

$$\Gamma_j(t)=\mathcal{N}\sum_{i=1}^{n} G_i(\mu_i,\sigma^2,t), \tag{3.9}$$

again with Gauss functions $G_i(\mu_i,\sigma^2,t)$ with random means μ_i and constant variances σ^2.

The applied dynamic fits are shown in Fig. 9 varying the assumed number of interacting modes and the different combinations of PCA modes as ground states. In the case of $M=2$ interacting modes [Fig. 9(a)] we recognize the deepest minimum with a combination of the first and second PCA mode. Dynamic fits with three and four interacting modes [Figs. 9(b) and 9(c)] show minima as well, but with higher values of V_d. A comparison of the best fits [Fig. 9(d)] presents the differences with respect to the number of interacting modes: the two-mode interaction is clearly detected.

Finally, we investigate the noisy Lorenz attractor (3.4). Dynamic fits are shown in Fig. 10 with varying number of interacting modes and PCA ground states. The investigation of two coupling modes leads to the 1-2 branch with minimal values; for three interacting modes the method neglects one noisy mode by combinations of the 1-2-4 PCA modes. A comparison of the best fits with $M=2$ and $M=3$ shows an interesting feature: though the Lorenz signal is determined by a three-dimensional set of differential equations our method detects a two-mode interaction: there is a deeper minimum for $M=2$. This is due to the similarity of the two amplitudes $x(t)$ and $y(t)$ [compare Fig. 5(a)] and the resulting correlation dimension $d_C=2.06$ of the Lorenz attractor [13]. The small differences between these two amplitudes cannot be resolved by our method in the presence of noise. However, the detection of two interacting modes and the

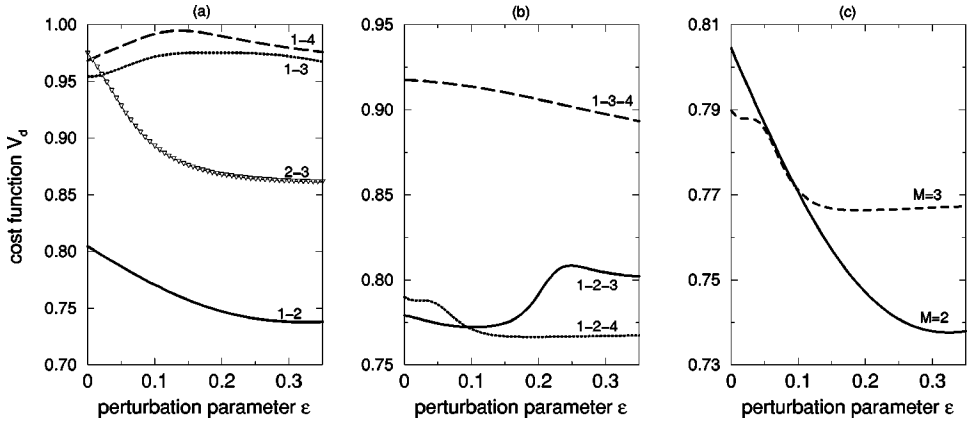

FIG. 10. Dynamic cost functions $V_d(M,\epsilon)$ calculated for the noisy Lorenz attractor, at various PCA ground states m-n. We recognize a best fit with the first two PCA modes as ground state (solid line) at M=2 (a) and a best fit with a PCA ground state built by modes 1, 2, and 4 (dotted line) at $M=3$, seen in (b). A comparison of the fits at $M=2$ and $M=3$ is presented in (c); a deeper minimum is found at $M=2$ (solid line), but the difference to the minimum at $M=3$ (dotted line) is quite small. PCA ground states at $M=1$ and $M=4$ are found at much higher values of V_d and are thus left out.

good correspondence to the exact solution (compare Fig. 8) is a considerable improvement compared to PCA approaches.

IV. CONCLUSIONS

We introduced a concept in nonlinear signal analysis for analyzing spatiotemporal signals. It considers signal dynamics beside a maximum signal representation. The idea mainly consists of an additional signal dynamics fit to a pure signal fit, interpreted as a perturbation of a PCA ground state. Introducing a biorthogonal basis, first-order perturbation leads to expansion coefficients of modes and polynoms of differential equations.

This approach improves PCA, since signal-noise separation is achieved even in the case of nonorthogonal signal and noise, and in the case of noise levels with larger contributions than signal contributions to the data. Finally, the number of interacting modes can be estimated by the presented algorithm.

The method is illustrated by examples of its application to simulated data sets: In the case of a noisy trajectory near a stable fixed point the dimensionality of the dynamics subspace is correctly estimated and a dramatic improvement compared to PCA is achieved. For a noisy three-dimensional chaotic signal embedded in a four-dimensional phase space the dimensionality is underestimated due to the fractal geometry of the attractor. However, the dominant structure of the attractor is reconstructed and noisy parts are separated.

The algorithm may represent a helpful tool for analyzing spatiotemporal signals in different fields of research.

[1] V. K. Jirsa and H. Haken, Phys. Rev. Lett. **77**, 962 (1996).
[2] A. V. Holden, M. Markus, and H. G. Othmer, *Nonlinear Wave Processes in Excitable Media* (Plenum Press, New York, 1991).
[3] G. Plaut and R. Vautard, J. Atmos. Sci. **51**, 210 (1994).
[4] M. Bestehorn, Phys. Rev. Lett. **76**, 46 (1996).
[5] R. Friedrich and C. Uhl, Physica D **98**, 171 (1996).
[6] A. Fuchs, J. A. S. Kelso, and H. Haken, Int. J. Bifurcation Chaos Appl. Sci. Eng. **2**, 917 (1992).
[7] C. Uhl, *Analysis of Neurophysiological Brain Functioning* (Springer-Verlag, Berlin, 1999).
[8] G. Berkooz, P. Holmes, and J. L. Lumley, Annu. Rev. Fluid Mech. **25**, 539 (1993).
[9] F. Kwasniok, Phys. Rev. E **55**, 5365 (1997).
[10] C. Uhl, R. Friedrich, and H. Haken, Phys. Rev. E **51**, 3890 (1995).
[11] D. R. Hartree, Proc. Cambridge Philos. Soc. **24**, 111 (1928).
[12] V. Fock, Z. Phys. **61**, 126 (1930); **62**, 795 (1930).
[13] H. G. Schuster, *Deterministic Chaos* (VCH-Verlag, Weinheim, 1995).